Enhancement CT Scan Image and Study Electronic, Structural and Vibrational Properties of Iobenguane

Ahlam Majead Kadhim, Huda M. Jawad, Shaimaa H. Abd muslim

Department of Physics, College of Science, Al-Mustansiriyah University

E-mail: drhuda222@uomustansiriyah.edu.iq, Shaimaamuslim@yahoo.com

Corresponding author: ahlammajead@uomustansiriyah.edu.iq

Abstract

The aim of this work is to provide general information about Iobenguane that can be used to obtain results to diagnose the diseases. Iobenguane, or MIBG, is an aralkylguanidine. When radiolabeled, it can be used in nuclear medicinal diagnostic techniques as well as in neuroendocrine antineoplastic treatments. This work is divided into two parts first part study electronic structure and vibration properties of the Iobenguane material. The second part study quality image enhancement techniques. CT scan image transformed to frequency domain using the LWT. Two contrast enhancement methods are applied to improve quality image properties; they are Histogram Equalization (HE) and Adaptive Histogram Equalization (AHE). Canny filter of edge detection used as a comparison tool between enhancement methods. The result show the absorbance of iobengaune in the range ($1000 - 0 \text{ cm}^{-1}$) of these single bonds from C-C, C-N, C-I, and C-O High absorbency and sharp peak of Maximum wavelength absorbed. From the results of measures quality like PSNR, mean and entropy indicate that the CT Scan images are enhanced obtained using AHE technique in frequency. The dark regions of enhanced CT Scan images became clarity comparing with input CT Scan image which is having low contrast.

تحسين الصورة المقطعي المحوسبة ودراسة الخصائص الإلكترونية والاهتزازية والهيكلية لـ Iobenguane

احلام مجيد كاظم، هدى محمد جواد، شيماء عبد مسلم

قسم الفيزياء، كلية العلوم، الجامعة المستنصرية

الخلاصة

الهدف من هذا العمل هو توفير معلومات عامة حول Iobenguane يمكن استخدامها للحصول على نتائج لتشخيص الأمراض. Iobenguane، أو MIBG، هو نظير aralkylguanidine. عند وضع العلامات الإشعاعية عليه، يمكن استخدامه في تقنيات التشخيص الطبي النووي وكذلك في علاجات الغدد الصم العصبية المضادة للأورام. ينقسم هذا العمل إلى جزئين: الجزء الأول يدرس التركيب الإلكتروني وخصائص اهتزاز مادة Iobenguane. الجزء الثاني يدرس تقنيات تحسين جودة الصورة. تم تحويل صورة المسح المقطعي المحوسب إلى مجال تردد باستخدام LWT. يتم تطبيق طريقتين لتحسين التباين لتحسين خصائص الصورة عالية الجودة ؛ هما معادلة الرسم البياني (HE) ومعادلة الرسم البياني التكيفي (AHE). يستخدم مرشح ماكر لاكتشاف الحواف

كأداة مقارنة بين طرق التحسين. تظهر النتيجة امتصاص iobengaune في النطاق (0-1000 سم$^{-1})$ لهذه الروابط المفردة من C-C و C-N و C-I و C-O الامتصاصية العالية والذروة الحادة من الطول الموجي الأقصى الممتص. من نتائج مقاييس الجودة مثل PSNR، يشير المتوسط والنتروبيا إلى أن صور التصوير المقطعي المحوسب قد تم الحصول عليها باستخدام تقنية AHE في التردد. أصبحت المناطق المظلمة لصور الأشعة المقطعية المحسّنة واضحة مقارنة بإدخال صورة التصوير المقطعي المحوسب ذات التباين المنخفض.

Introduction

Imaging technology is one of the techniques used in computerized tomography (CT Scan) which generates three-dimensional images of human body tissues. X-ray scans pictures provide detailed information of an object such as dimensions shape and density. Quality of these CT Scan images need to be improve because the process of obtaining these images is accompanied by camera spread, noise, and reflection of X-rays [1]. Iobenguane I -131 has like construction Iobenguane to the neurotransmitter norepinephrine and self-accumulation pathways and uptake as norepinephrine. Transporters in adrenergic nerve terminals and accumulates in adrenergic ally innervated tissues, such as the heart, lungs, adrenal medulla, salivary glands, liver, and spleen, as well as in tumors that originate in the neural crest. Following intravenous administration, iobenguane I-131 is taken up by and accumulates into paraganglioma cells and pheochromocytoma; radiation resulting of radioactive decay of I-131 causes cell death and tumor necrosis. Iobenguane I-131 should be taken within the control of physicians that are qualified by particular training and experience in the handling experience and safe use. (MIBG) is followed, after varying period, by images of the whole body. The purpose is to detect tumors. Either Iodine at the meta position. The uptake mechanism is based on specific characteristics of abnormal neural crest cells [2]. Physical properties were investigated using density functional theory the basis set B3LYP (Becke 3-Lee-Yang-Parr) /3-21G [3].

Basis set that generated by Gaussian 09 program to investigating the molecular shape, length of the bond, and angles like dihedrals is molecular geometry. Nuclear Magnetic Resonance, ultraviolet rays and infrared spectra: these can be predicted [4]. In theoretical chemistry collective between mathematical methods and fundamental laws of physics to study processes of chemical relevance [5, 6]. Engineering and sciences can be used widely and successfully applied in simulations of electronic structure by use Density Functional Theory [7]. Fig.1 represent the geometrically structure of Iobengaune with chemical formula ($C_8H_{10}IN_3$) and iodine isotopic (I131) [8].
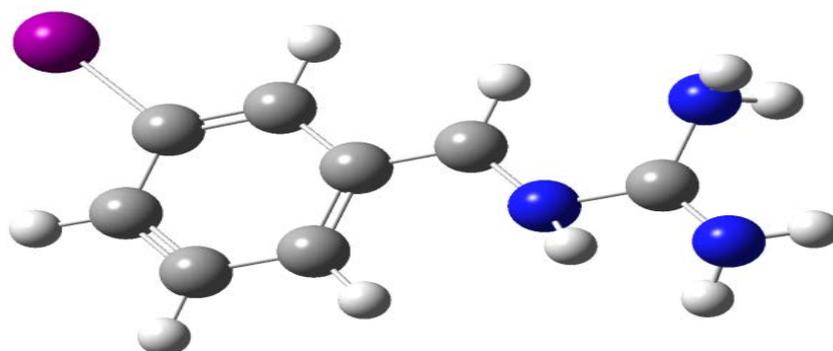

Fig.1: Geometrically optimized of structure of Iobengaune.

(Sabrina et al 2019) stated that (iobenguane I-131) is the first and only FDA-approved therapeutic drug to treat patients with unrespectable, locally advanced, or metastatic rare tumors of the adrenal gland, pheochromocy atoms and paragangliomas [9]. D.L.et al. 2020 determined iobenguane I-131 maximum permissible dose for children with neuroblastoma secondary goals for assessing the overall response and dosing the tumor and organs [10]. Teh, et al. 2018 proposed new histogram modulation technique (GCAELEWD) that could provide good contrast to highlight the region of interest. This new technique is used to increase the difference in the severity of brain CT images [11]. (Siracusano, et al. 2020). Proposed a new technique to improve chest X-ray sensitivity via a nonlinear post processing tool, called PACE, which correctly combines a (FABEMD) with (CLHE). The results show that this method is effective for improving CT Scan image [12].

Wavelet transformations

Discrete wavelet transform (DWT) analyzes image signal to the wavelet coefficients that can be remove some details like noise. The image is analyzed to four sub band images (cA, cH, cV and cD) by preforming the DWT first level into frequency domain [10, 11]. Lifting Wavelet Transform (LWT) is introduced to fast DWT; this is easily achieved by the computer due to the great reduction in calculations [13]. This approach is totally based on the spatial performance of the DWT [14].

Image Enhancement techniques

In this research, the methods used for image enhancement are histogram equalization (HE) and adaptive equalization histogram (AHE). In applying these methods, Red, Green, and Blue channels in RGB images can produce dramatic changes in image color balance because the relative distribution of the color channel changes relatively. Thus, it is an important stage to convert color images into gray scale images. Edge detection is an important stage in pattern recognition and medical image analysis techniques. Classical edge detection are not practical in medical image processing, because the high sensitivity to noise. Classical edge detection techniques preform local operators to approximately calculate the first derivative of gray image gradient of an image in the spatial domain, like Canny operator and Sobel operator. In this work, the LWT and Canny operator based on edge detection technique is discussed [15].

Histogram Equalization (HE)

Adjusting the light density value can be performed by using HE to enhance image contrast. HE includes replacing the light density data values so output image histogram identifies to convenient histogram. The basic concept of HE is to remap the data value of the light density value for the processed image with a new value data of light density through the transformation function as in the following equation [16].

$$S_k = \frac{(n_G - 1)}{n} \sum_{j=0}^{k} n_{rj} \qquad (1)$$

where S_k is the Gray levels number, n is the mage pixels number and n_{rj} is the pixels number of rj gray level.

This technique is a flatter dynamic range of histogram image and the output is the enhancement of contrast image. HE safely changes lightness input image and makes some regions very shining or very dark [16].

Adaptive Histogram Equalization (AHE)

The contrast operator works to prevent too much saturation within homogeneous image regions depicted as high peaks in specific image histogram. Contrast can be limited to averting noise which accompanies the image. Image contrast is raised using AHE with changing the value of image data lighting. If (r) represents image gray level to be increased and T the conversion function, the converted value (S) calculated as follows [17]

$$S = T(r) = \int_0^r P_r(W)dw \qquad (2)$$

where P_r and P_s are the function of the probability density functions of r and s. Then P_s can be obtained by applying Eq.(4) as follows:

$$P_s(S) = P_r(r)\left|\frac{dr}{ds}\right| \qquad (3)$$

The proposed method

Medical CT Scan image used in this work is an image of the upper part of the body of an old patient woman (head, upper limbs and thorax). Medical CT Scan has been captured by the device in the Medical City hospital in Baghdad. The medical image under study in this research is illustrated within the first row in Fig.2. The resulted enhanced images of the AHE technique was converted to binary image of the color (0, 1) using Canny operator technique to poetizes edge detection with measures returning the most points edges and reduces the error mean. After this step Canny operator mark only the edge regions in white color. Canny operator detected the edge by separating noise from the image before detecting the edge of the image without changing the edge properties of CT Scan image and finding the threshold peak value of Canny operator.

Enhancement Algorithm Using LWT

The LWT conversion is applied to convert medical image to the frequency domain and the output is five images for the LWT coefficients for each enhancement techniques as illustrated in Fig.2. Fig.3 shows the complete programing stages of implementing the proposed contrast enhancement algorithm.
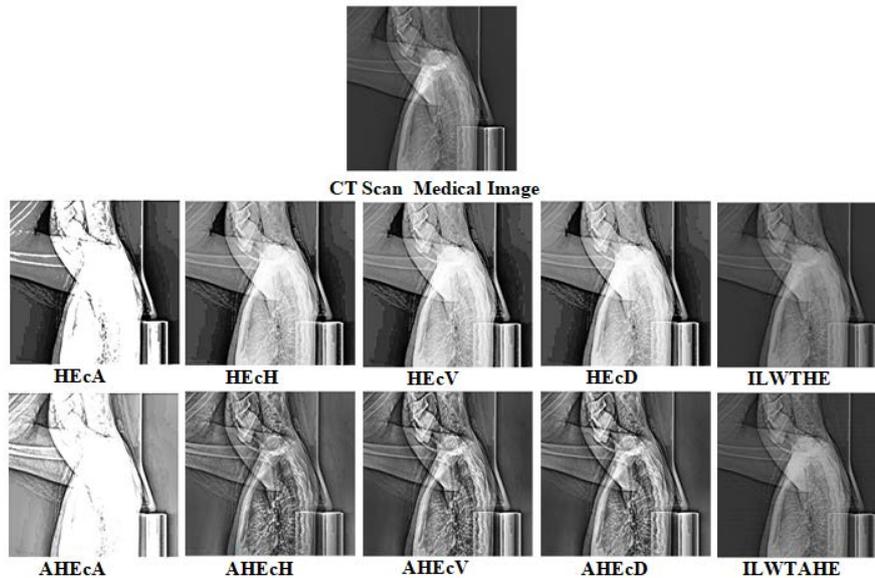
Fig.2: Enhanced CT Scan images for all coefficients used HE and AHE techniques.

The stepes of proposed algorithim are explain within the following steps:

Input: Medical CT-Scan image.

Output: Enhanced CT-Scan images.

Step1: Input and read CT Scan image.

Step2: Preform LWT for input image to get four coefficients matrices.

$$[\,cA\,,cH\,,cV\,,cD] \leftarrow LWT(CT\ Scan)$$

Step3 Resize the resulted coefficients matrices to the size of input image.

Step4: Each one of coefficients matrices output from step 3 is added to an input image.

$$cACT \leftarrow CT\ San + cA$$

$$cHCT \leftarrow CT\ San + cH$$

$$cVCT \leftarrow CT\ San + cV$$

$$cDCT \leftarrow CT\ San + cD$$

Step5: Analyzing each one of the four coefficients matrices to their component channels color RGB.

Step6: Perform HE for each channels, then collected RGB images to get the output coefficients of the enhanced image.

$$HEcA \leftarrow HE(R, G, B\ of\ cACT)$$

$$HEcH \leftarrow HE(R, G, B\ of\ cHCT)$$

$$HEcV \leftarrow HE(R, G, B\ of\ cVCT)$$

$$HEcD \leftarrow HE(R, G, B\ of\ cDCT)$$

Step7: Perform AHE to get enhanced image for AHE technique.

$$AHEcA \leftarrow AHE(R, G, B\ of\ cA)$$

$$AHEcH \leftarrow AHE(R, G, B\ of\ cH)$$

AHEcV ← **AHE(R, G, B of cV)**

AHEcD ← **AHE(R, G, B of cD)**

Step8: Preform invers LWT to get two enhanced images.

ILWTHE ← **[cA , HEcH , HEcV , HEcD]**

ILWTAHE ← **[cA , AHEcH, AHEcV, AHEcD]**

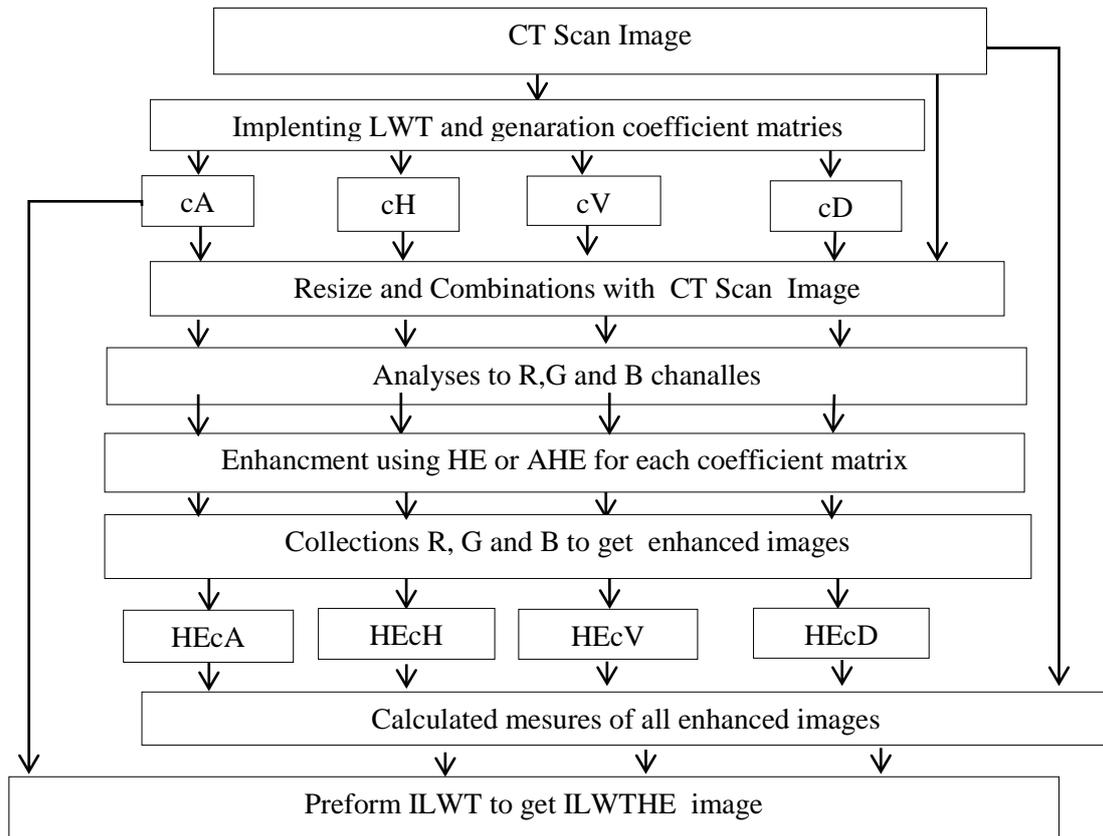**Step9:** Calculate the measures (Mean, Entropy and PSNR) for all enhanced images.

Fig.3: Flow chart of the proposed algorithm.

HE and AHE are applied to all coefficients image resulted from the LWT. Edges detection using Canny filter is made for the enhanced images resulted after applying AHE for all coefficients image, see Fig.4. a comparison between the enhanced images from both techniques HE and AHE is made, to decide on the best enhanced image to distinguishing medical CT Scan image for the human body.

Quality measures

Table 1 shows the results of the quality measures. Quality measures mean and entropy produced results values of the original approach to their values, and this results using AHE technique is better than the use of HE, this fact is evident through the results of the peak signal to noise ratio (Psnr) that are shown in Table 1. Psnr measure is calculated using follow equation:

$$PSNR = 20 \log 10 \left(\frac{2^{Bps-1}}{\sqrt{MSE}} \right) \qquad (4)$$

MSE is the mean square error of signal. The default for BPS is 8, so the maximum possible pixel value of an image is 255. It can be concluded that the enhanced image contained high frequency of LWT especially cH, cV and cD are more suitable to get enhanced CT Scan image. Fig.4 shows histogram and edge detection result after performing AHE within frequency domain using LWT function comparing with edge detection for the original CT Scan image. It is noticed that the detail of output images regions looks clearer than the image before enhancement this is an evidence of getting more specifics and details with distinguishable different objects in same image vision.
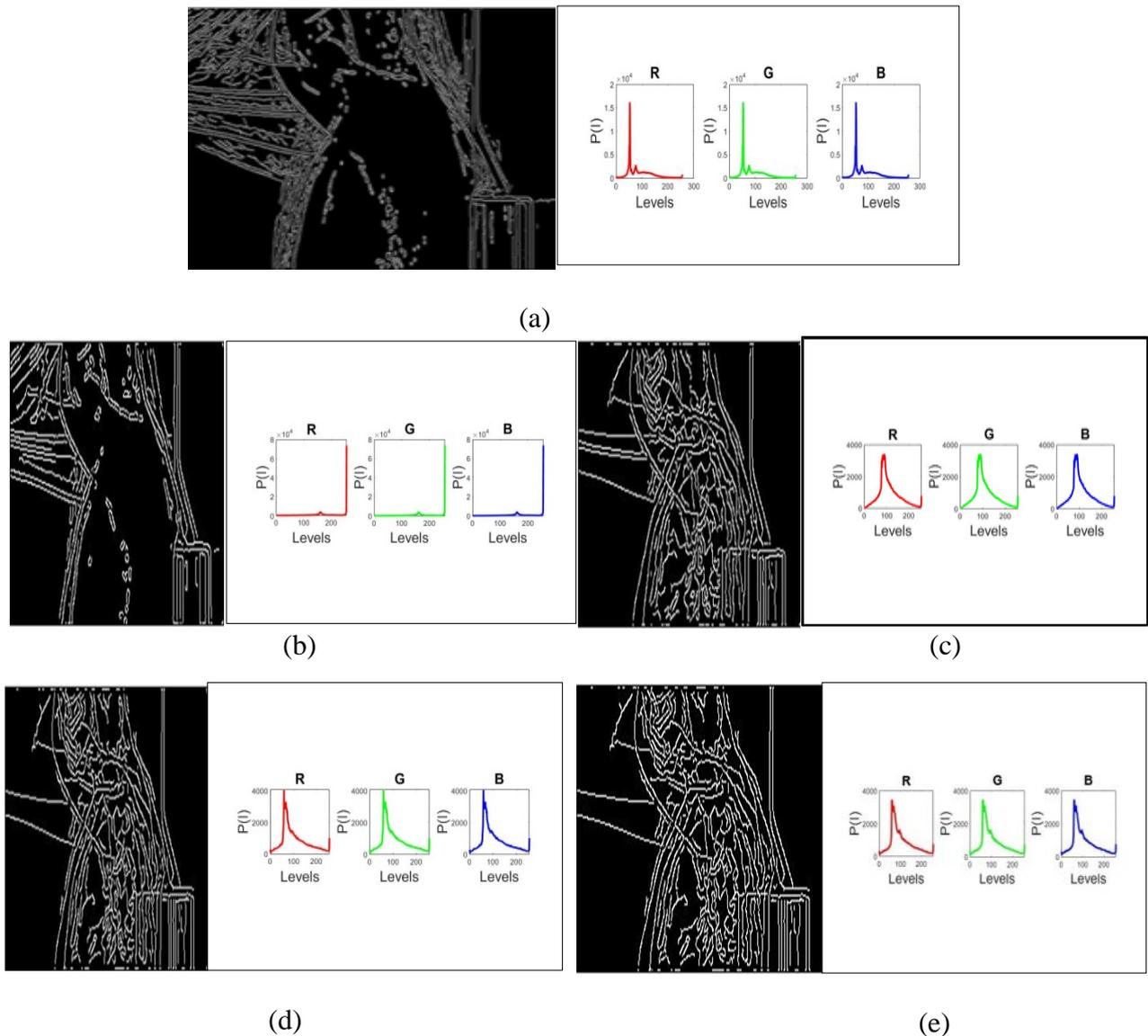

(a)

(b)

(c)

(d)

(e)

Fig.4: Canny edges detection results and histogram for the images: (a) CT Scan image, (b) AHEcA, (c) AHEcH, (d) AHEcV and (e) AHEcD.

Table 1: Results measures of CT-Scan image.

Images	mean	entropy	Psnr
CT Scan	86.7229	6.8955	
		HE Results	
HEcA	196.8206	3.7769	10.7702
HEcH	127.4204	5.6031	13.7285

HEcV	127.4477	5.5776	13.7163
HEcD	127.6242	5.5766	13.3714
ILWTHE	84.8207	7.0988	11.0594
		AHE Results	
AHEcA	149.4683	5.2177	11.9792
AHEcH	110.1898	7.3856	17.2078
AHEcV	104.9244	7.5381	18.5609
AHEcD	104.9707	7.5402	18.2925
ILWTAHE	84.6682	7.1079	11.1197

Iobenguane absorbances

I-131 MIBG was observed in the primary tumor, Intensity of I-131 MIBG uptake can be similar in benign and malignant tumors. Rising tracer absorbance is linked either to bone metastases or to bone marrow infiltration or both [18]. Structure information of a molecule can be obtained by analyzing the infrared spectrum. Fig.5 shows absorbance of iobenguane. The range $(1000 – 0$ $cm^{-1})$ of single bonds from C-C, C-N, C-Iand C-O High absorbency and sharp peak. At 1600 cm^{-1} sharp peak for C=C double bond and $(2900$ $cm^{-1})$ C-H The carbon atom has a hybrid type SP^3. Either $(3100$ $cm^{-1})$ C-H The carbon atom has a hybrid type SP^2 then 3300 for N-H symmetry and 3400 cm^{-1} for N-H asymmetry because asymmetric energy is greater than symmetry energy [19].
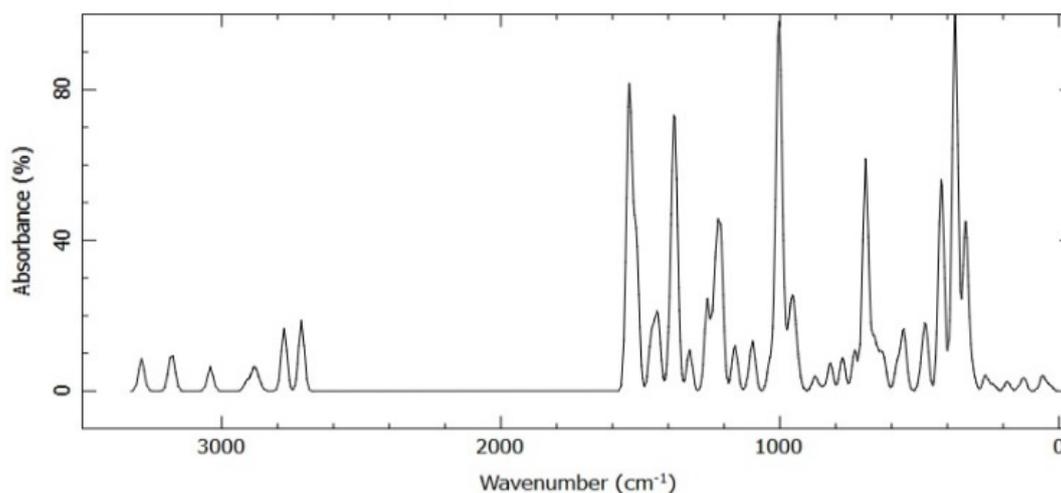

Fig.5: Absorbance of Iobengaune.

In some areas of the near ultraviolet and visible regions the substances will absorb light electronic transitions occur and these include vibrational transitions in the infrared and rotational transitions in the microwave regions. The data is used to produce absorbance spectra. An optical spectrometer records the wavelengths at which absorption occurs and the degree of absorption for each wavelength to produce a spectrum [19]. Fig.6 shows UV- visible to Iobengaune between epsilon means constant called malar absorptivity and excitation energy.
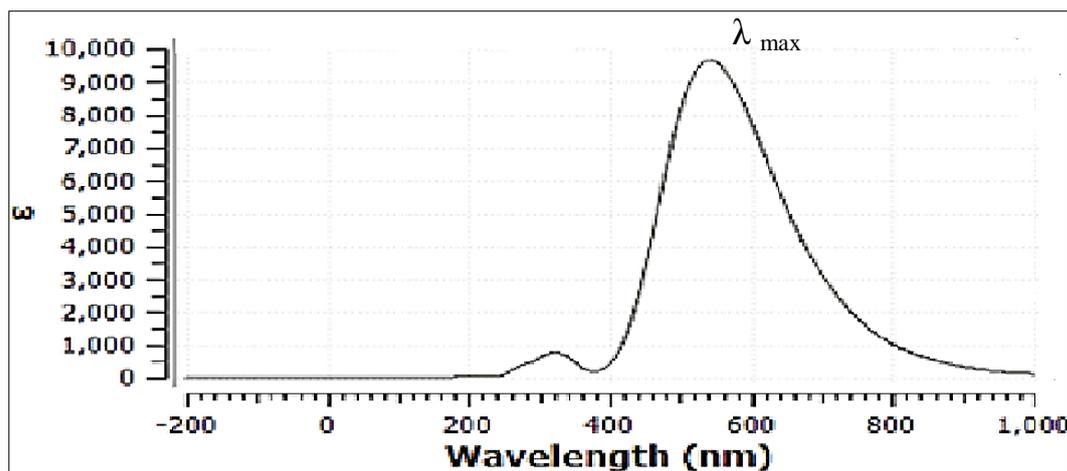
Fig.6: UV- visible spectrum of Iobengaune.

λ_{max} is the wavelength where maximum absorption occurred. The maximum wavelength absorbed is at (640.66 nm) and the biggest energy is (1.9353 eV). The half width is (0.333 eV) at half height is (2685.83cm^{-1}). Both λ_{max} and ε (molar absorptivity) increases with the increase of conjugation. In this figure two peaks are noted means that there is benzene ring Iobengaune electrostatic potential surfaces were calculated using the density functional theory method with the exchange part and the B3LYP. [20]. Molecular electrostatic potential surfaces (MESP) are useful for understanding the relationship between biological activity and molecular structure. Fig.7 represents an Iobengaune electrostatic potential surface. Negative values indicate (tending to red) of electrostatic potential - regions more electrons, in the case of molecule are more electronegative is composed of nitrogen atoms (tending to blue) representing electron deficiency were especially marked in rings benzene compounds exclusively of hydrogen and carbon atoms (focusing on areas of carbon), establishing this area as more electropositive [20].
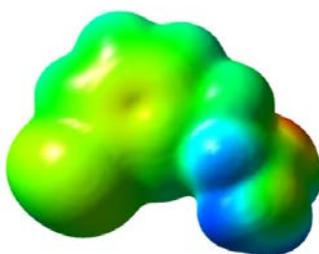

Fig.7: Electrostatic potential surfaces of Iobengaune.

Conclusions

From observing edges detection of improved images in frequency domains it can be concluded that AHE a good result in clearing the details of the CT Scan image and separating the different image regions, but the coefficients matrices cH, cV and cD produced the best enhanced images. Iobengaune absorbance is in the range (1000 – 0 cm^{-1}) of these single bonds from C-C, C-N, C-I, and C-O High absorbency and sharp peak. Maximum wavelength absorbed (640.66 nm) and the biggest energy (1.9353 eV). The half width is (0.333 eV) at half height is (2685.83 cm^{-1}). Electrostatic potential, electron deficiency were especially marked in rings benzene compounds exclusively of carbon and hydrogen atoms (focusing on areas of carbon), establishing this area as more.

References

[1] D.L. Bailey, J.L. Humm, A. Todd-Pokropek, A. Van Aswegen, "Nuclear Medicine Physics A Handbook for Teachers and Students", 2014.

[2] Matthew Stenger, "Iobenguane I-131 for Advanced Pheochromocytoma or Paraganglioma", November 25, 2018.

[3] Erik De Clercq, Hugh J. Field, British Journal of Pharmacology, 147, 1 (2006) 1-11.

[4] Errol G. Lewars, "Computational Chemistry Introduction to the Theory and Applications of Molecular and Quantum Mechanics", 2011.

[5] Frank Jensen, "Introduction to Computational Chemistry", Wiley, 2006.

[6] Andrew Gilbert, "Introduction to Computational Chemistry Theory", Rm 118, Craig Building, RSC, 2011.

[7] G. Robert, Parr, Yang, Weitao, "Density Functional Theory of Atoms and Molecules", Oxford University Press, Oxford, 1994.

[8] Aron J. Cohen, Paula Mori-Sánchez, Weitao Yang, Science, 321, 5890 (2008) 792-794.

[9] Sabrina Abdullaeva, Crystal Botkin, Sarah Frye, Razi Muzaffar, Medhat Osman, Journal of Nuclear Medicine, 60, 1 (2019) 2046.

[10] Pierre Olivier, Paula Colarinha, Jure Fettich, Sibylle Fischer, Jörgen Frökier, Francesco Giammarile, Isky Gordon, Klaus Hahn, Levent Kabasakal, Mike Mann, Mercedes Mitjavila, Amy Piepsz, Ute Porn, RuneSixt, Jeannette Van Velzen, European Journal of Nuclear Medicine and Molecular Imaging, 30 (2002) B45–B50.

[11] V. Teh, K. S. Sim, E. K. Wong, International Journal of Innovative Computing, Information and Control, 14, 3 (2018) 1029-1041.

[12] G. Siracusano, A. La Corte, M. Gaeta, G. Cicero, M. Chiappini, G. Finocchio, arXiv preprint arXiv:2006.04149 (2020) 1-17.

[13] J. Petrova and E. Hostalkova, Czech Repuplic, (2001) 1-5.

[14] C.-C. Lai and C.-C. Tsai, IEEE Trans. Instrum. Meas, 11, 59 (2010) 3060-3063.

[15] Tinku Acharya, Chaitali Chakraabati. Springer, 42, 3 (2006) 321-339.

[16] Ingrid Daubechies, Wim Sweldens, NSF (grant DMS-9401785) Princeton University, Princeton, New Jersey, 1996.

[17] Erwin, Saparudin, A. Nevriyanto, D. Purnamasari, Proceedings of the International MultiConference of Engineers and Computer Scientists, 2018 (2018) 157-163.

[18] Rancesco Giammarile, Isky Gordon, Klaus Hahn, Levent Kabasakal, Mike Mann, Mercedes Mitjavila, Amy Piepsz, Ute Porn, RuneSixt, Jeannette Van Velzen. "Guideline for Radioiodinated MIBG Scitnigraphy in Children", 2002.

[19] Barbara Stuart, "Infrared Spectroscopy: Fundamentals and Applications", John Wiley & Sons, Ltd, 2004.

[20] Hinna Hamid, "Ultraviolet and Visible Spectrophotometry", New Delhi, 2007.